267/99 Submitted to JOSA - 2002

An efficient inverse scattering algorithm for the design of grating-assisted codirectional mode-couplers

Ricardo Feced, Michalis N. Zervas

Optoelectronics Research Centre,
University of Southampton,
Southampton SO17 1BJ (UK)

An efficient inverse scattering algorithm for the design of grating-assisted codirectional mode-couplers

Abstract

This paper presents an efficient method for the design of optical devices based on codirectional grating-assisted mode-coupling. A low complexity algorithm is developed to calculate the coupling function of a grating that accurately matches an arbitrarily given target spectral response. The method relies on the synthesis of the grating impulse response by means of an exact differential layer-peeling algorithm.

1. Introduction

The principle of operation of many practical optical filters rely on grating assisted coupling between two different modes of an optical waveguide [1-3]. These optical devices can be classified attending to the nature of both the interacting optical modes and the grating. Two broad groups can be distinguished according to the direction of propagation of the optical modes: contradirectional couplers, if the modes propagate in opposite directions; and codirectional couplers, if they copropagate along the waveguide. The field of fibre optics provides examples for both types of devices. Fibre Bragg gratings, for instance, couple forward and backward propagating modes of the fibre, and have become key components for many optical communication systems [4]. Examples of Grating Assisted Codirectional Couplers (GACC) include long period gratings, which couple guided modes to cladding and radiation modes [5]; polarisation couplers, which couple light between two orthogonal polarisation modes [6]; and spatial mode convertors, that couple light between different spatial modes of the optical waveguide [7].

A problem of great practical importance is that of designing the appropriate grating to achieve a desired filter spectral response. Electromagnetic inverse scattering techniques have been extensively used for this purpose [8]. The simplest approach exploits the approximate Fourier transform relation that exists between the filter spectral response and the grating coupling function [9-11]. However, this synthesis procedure is not reliable for the design of filters with strong mode-coupling. A second group of inverse scattering methods is that of exact solutions expressed in terms of the Gelfand-Levitan-Marchenko (GLM) integral equations [12]. The main drawback of this approach is the difficulty involved in solving the GLM equations in the general case. If the spectral response is approximated by rational functions, then analytical solutions can be obtained [13-15]. This requirement is, however, too restrictive in practice and alternative iterative solutions to the GLM equations have been proposed to overcome it [16]. The two main weaknesses of these iterative solutions are their slow convergence for strongly coupled filters and also their low algorithm efficiency, with a complexity that scales as $O(N^3)$, where N is the number of points in the grating.

Other synthesis methods are based on optimisation algorithms that attempt to minimise the error between the target spectral response and that of the designed grating. Strategies that rely on variational optimisation [17] and genetic algorithms [18] have been described in the literature. These techniques suffer in a more pronounced way of slow convergence and low algorithmic efficiency when applied to the design of complex gratings. This is a natural consequence of the great number of degrees of freedom involved in the grating design optimisation problem.

There exists a third group of exact inverse scattering algorithms called differential or direct methods [19,20]. These techniques exploit fully the physical properties and structure of the layered media in which the waves propagate. The methods are based on causality arguments, and identify the medium recursively layer by layer. The main advantage of these layer-peeling methods is their low algorithmic complexity, which grows only as $O(N^2)$. Recently we have presented a differential algorithm for the synthesis of complex contradirectional gratings [21]. The purpose of this paper is to develop a parallel methodology to design optical filters based on codirectional grating-assisted coupling. We will show that this case exhibits certain differences with respect to the contradirectional one, but that the same algorithm can be applied if it is properly extended and modified. The paper is structured as follows: Section 2 studies the properties of the transfer functions of grating assisted codirectional couplers (GACC); Section 3 will describe the design methodology; and Section 4 will finally present some results of grating reconstruction and synthesis.

2. Transfer functions for codirectional grating-assisted couplers

In this section we study the properties of the spectral response of GACCs. We will first introduce the coupled-mode formalism as a tool to analyse this type of devices. Then we will discretise the propagation problem and discuss the properties of the GACC transfer functions in the light of digital signal processing techniques. This study is necessary to define a well-posed inverse scattering problem that guarantees the existence and uniqueness of the sought grating coupling function.

2.1 Coupled-mode formalism

GACCs rely on the resonant exchange of power between two different modes of an optical waveguide that interact through a periodic grating. The electromagnetic properties of lossless GACCs are usually described by a reference period for the grating Λ (with $K_o = 2\pi/\Lambda$), and a slowly z-varying complex function q(z) that modulates the amplitude and phase of the mode-coupling.

- **Space-frequency (z-β) coupled-mode formulation:**

The propagation equations that describe the interaction of the modes with the grating can be written in terms of the coupling function q(z) for the grating and the amplitudes of the two interacting modes: the slow mode $b_S(z,\beta)$, and the fast mode $b_F(z,\beta)$ [22,1-3].

$$\begin{aligned} \frac{db_S(z,\beta)}{dz} - j\beta\, b_S(z,\beta) &= -q(z)^*\, b_F(z,\beta) \\ \frac{db_F(z,\beta)}{dz} + j\beta\, b_F(z,\beta) &= q(z)\, b_S(z,\beta) \end{aligned} \tag{1}$$

where β is the detuning parameter:

$$\beta(\omega) = \frac{\beta_S(\omega) - \beta_F(\omega) - K_o}{2} \approx \left.\frac{\partial(\beta_S - \beta_F)}{\partial\omega}\right|_{\omega_o} \frac{\omega - \omega_o}{2} \equiv \frac{\Delta n_{eff}}{c}\pi\left(f - f_o\right) \tag{2}$$

and the following variables have been introduced: ω is the optical angular frequency; $\beta_S(\omega)$ and $\beta_F(\omega)$ are the propagation constants for the slow (S) and fast (F) modes; ω_o is the resonance angular frequency ($\beta_S(\omega_o)$-$\beta_F(\omega_o)$=K_o); Δn_{eff} is an effective refractive index difference between the S and F modes; c is the speed of light in vacuum; and f is the optical frequency.

The actual electric fields ($e_S(z,\beta)$ and $e_F(z,\beta)$) are related to the waves $b_S(z,\beta)$ and $b_F(z,\beta)$ through the expressions:

$$\begin{aligned} e_S(z,\beta) &= b_S(z,\beta)\, e^{j\frac{\beta_S(\omega)+\beta_F(\omega)}{2}z}\, e^{+j\frac{K_o z}{2}} \\ e_F(z,\beta) &= b_F(z,\beta)\, e^{j\frac{\beta_S(\omega)+\beta_F(\omega)}{2}z}\, e^{-j\frac{K_o z}{2}} \end{aligned} \tag{3}$$

- **Space-time (z-τ) coupled-mode formulation:**

The equations (1) and (2) describe the scattering problem in the space-frequency (z-β) domain. The propagation system can be Fourier transformed ($\beta \leftrightarrow \tau$) to yield the following space-time (z-τ) partial differential equation system:

$$
\begin{aligned}
\frac{\partial b_S(z,\tau)}{\partial z} + \frac{\partial b_S(z,\tau)}{\partial \tau} &= -q^*(z)\, b_F(z,\tau) \\
\frac{\partial b_F(z,\tau)}{\partial z} - \frac{\partial b_F(z,\tau)}{\partial \tau} &= q(z)\, b_S(z,\tau)
\end{aligned}
\qquad (4)
$$

The system of equations (4) describes the propagation problem in a reference frame moving with a speed equal to the average group velocity between both interacting modes. The variable τ measures time-delay in spatial units, and can be converted into real time through the expression:

$$
t = \frac{\beta\, \tau}{\omega - \omega_0} = \frac{\Delta n_{eff}}{2c}\, \tau \qquad (5)
$$

- **Transfer matrix**

The solution of the coupled-mode equations (1) yields the spectral transfer functions that describe the GACC filter. They can be written in the space-frequency domain as elements of the following transfer matrix:

$$
\begin{bmatrix} b_S(L,\beta) \\ b_F(L,\beta) \end{bmatrix} = \begin{bmatrix} T_{SS}(\beta) & T_{SF}(\beta) \\ T_{FS}(\beta) & T_{FF}(\beta) \end{bmatrix} \begin{bmatrix} b_S(0,\beta) \\ b_F(0,\beta) \end{bmatrix} \qquad (6)
$$

The elements of this transfer matrix satisfy the following properties:

$$
T_{FF}(\beta) = T^*_{SS}(\beta) \qquad (7.1)
$$

$$
T_{SF}(\beta) = -T^*_{FS}(\beta) \qquad (7.2)
$$

$$
|T_{SF}(\beta)|^2 + |T_{FF}(\beta)|^2 = 1 \qquad (7.3)
$$

The last property (7.3) is a consequence of the power conservation principle. If we assume that the GACC in Figure 1 is excited through port 1 (fast mode), then the element $T_{SF}(\beta)$ will give the filter's spectral response when the output signal is monitored at port 4 (slow mode). Performing a Fourier transform ($\beta \leftrightarrow \tau$) on equation (6), we can express the solution for the space-time propagation problem (4) as a convolution integral of the time-transformed transfer matrix $T_{ij}(\tau)$ with the input waves $b_{S(F)}(0,\tau)$. The inverse scattering methodology that we are going to develop will enable us to obtain the coupling function q(z) required to obtain a target spectral response for $T_{SF}(\beta)$.

2.2 Discretisation of the propagation problem

We will discretise the propagation problem by dividing the grating into a number of sections of uniform coupling constant q and fixed length Δ. The transfer matrix (6) for each of these sections is expressed through the well known matrix $M_T(\Delta,\beta)$:

$$\begin{bmatrix} b_S(z+\Delta,\beta) \\ b_F(z+\Delta,\beta) \end{bmatrix} = \underbrace{\begin{bmatrix} \cos(\xi\Delta)+j\frac{\beta}{\xi}\sin(\xi\Delta) & -\frac{q^*}{\xi}\sin(\xi\Delta) \\ \frac{q}{\xi}\sin(\xi\Delta) & \cos(\xi\Delta)-j\frac{\beta}{\xi}\sin(\xi\Delta) \end{bmatrix}}_{M_T(\Delta,\beta)} \begin{bmatrix} b_S(z,\beta) \\ b_F(z,\beta) \end{bmatrix} \tag{8}$$

where $\xi^2 = |q|^2 + \beta^2$. We can approximately factor $M_T(\Delta,\beta)$ as the product of a localised and instantaneous mode-coupling matrix $M_C(\Delta,q)$ and two propagation matrices $M_P(\Delta/2,\beta)$:

$$M_T(\Delta,\beta) \approx \underbrace{\begin{bmatrix} e^{j\frac{\beta\Delta}{2}} & 0 \\ 0 & e^{-j\frac{\beta\Delta}{2}} \end{bmatrix}}_{M_P\left(\frac{\Delta}{2},\beta\right)} \underbrace{\begin{bmatrix} \cos(|q|\Delta) & -\frac{q^*}{|q|}\sin(|q|\Delta) \\ \frac{q}{|q|}\sin(|q|\Delta) & \cos(|q|\Delta) \end{bmatrix}}_{M_C(\Delta,q)} \underbrace{\begin{bmatrix} e^{j\frac{\beta\Delta}{2}} & 0 \\ 0 & e^{-j\frac{\beta\Delta}{2}} \end{bmatrix}}_{M_P\left(\frac{\Delta}{2},\beta\right)} \tag{9}$$

The error involved in the approximation (9) is of the order $O(\Delta^3)$, and has been shown to be negligible if a small enough value for the grid size Δ is selected [21].

The transfer matrix corresponding to the whole grating will be written as the product of mode-coupling M_C and propagation matrices M_P. The propagation matrices account for the relative time-delay between the two interacting modes due to their different groups velocities. We can visualise the propagation through the grating by means of the space-time (z-τ) diagram that appears in Figure 2a. This figure also shows a digital lattice-filter with a response equivalent to the discrete GACC (Figure 2b). This lattice filter consists of the concatenation of coupling-matrices (M_C) and time-delays τ of value Δ (M_P).

In order to study the analytical properties of the transfer matrices it is useful to change the moving reference frame, and measure delays with respect to the propagation time of the fast mode. In this case the space-time characteristics for the fast mode are horizontal lines as illustrated in Figure 3a. Consequently, the digital lattice realisation of the filter will exhibit time-delays ($\tau = 2\Delta$) only along the path of the slow mode (Figure 3b). Now we are ready to analyse the GACC using standard techniques of digital signal processing like, for instance, the Z-transform [23,24].

2.3 Properties of the GACC transfer functions

The discretisation procedure introduced in the last section permits us to study GACCs by means of the Z-transformed transfer functions $T_{SF}(Z)$ and $T_{FF}(Z)$ of their equivalent lattice filter [23]. Digital filters are completely characterised by specifying the position of the poles and zeros of their transfer functions together with their region of convergence in the complex plane. As the lattice filter in Figure 3 belongs to the Finite Impulse Response (FIR) type, neither of the transfer functions $T_{SF}(Z)$ or $T_{FF}(Z)$ will contain any poles, except possibly at Z=0. With regard to their zeros, there is in principle no restriction for the position of the zeros for the transfer function $T_{SF}(Z)$. Some of them could be outside the unit circle, others on the same circle, and the rest inside it. The zeros of the $T_{FF}(Z)$ transfer function, on the contrary, have to obey certain restrictions in the limiting case of very weak coupling, i.e. when $\varepsilon = \max\{|q(z)|\} \to 0$. In this case all the zeros of $T_{FF}(Z)$ must be within the unit circle, and $T_{FF}(Z)$ is a causal and minimum-phase function. We can easily prove this by noticing that in this limit $T_{FF}(Z)$ tends to:

$$T_{FF}(Z) \to 1 + \varepsilon^2 \sum_{n=0}^{N} a_n Z^{-n} \qquad (10)$$

where N and a_n are finite numbers that depend on the structure discretisation. The ε^2 dependence in the sumatory term is due to the fact that at least two scattering events are necessary for a propagation path to contribute to this term of the $T_{FF}(Z)$ transfer function. We observe that the zeros of $T_{FF}(Z)$ tend to Z=0 in this limit, and that most of the light is directly transmitted to the output port 3 without suffering any scattering.

If the modulus of the coupling function q(z) is gradually increased, some of the zeros of $T_{FF}(Z)$ will move towards the unit circle, and eventually one of them will cross it. At this point there is a frequency for which the GACC couples all the power from the fast mode to the slow mode. Attending to the position of the zeros of $T_{FF}(Z)$, we can classify GACCs in several different types. We will say that the coupler is undercoupled if $T_{FF}(Z)$ has no zeros outside the unit circle, and overcoupled in the opposite case. We can also define a degree of overcoupling as the number of zeros that $T_{FF}(Z)$ has outside the unit circle.

To illustrate these properties let us consider a uniform GACC of constant length L, and increase gradually its coupling coefficient q. In this particular example, we have discretised the grating in 63 sections and, consequently $T_{FF}(Z)$ will also have 63 zeros. Figure 4 shows the zero-diagram in the complex plane for the following values of the product qL: $10^{-150}\cdot(\pi/2)$, $0.5\cdot(\pi/2)$, $1\cdot(\pi/2)$, $2\cdot(\pi/2)$, $3\cdot(\pi/2)$, and $8\cdot(\pi/2)$. We observe that for qL less than $(\pi/2)$ the filter is undercoupled; for $(\pi/2)<qL<3\cdot(\pi/2)$, the filter is overcoupled of degree 1; and, in general, for $(2n-1)\cdot(\pi/2) < qL<(2n+1)\cdot(\pi/2)$ the degree of overcoupling is n.

3. Inverse scattering method

In this section we will describe a procedure to calculate the coupling function q(z) that corresponds to an arbitrarily specified spectral response $T_{SF}(\beta)$. This inverse scattering problem has not a unique solution and the sought grating profile will depend on the selected function for $T_{FF}(\beta)$. We will present an algorithm that yields an optimum grating design in the sense that achieves the desired $T_{SF}(\beta)$ with an undercoupled filter, this is, minimising the value of the coupling function $|q(z)|$.

3.1 The equivalent contradirectional problem

By inspecting Figure 2 we observe that the codirectional coupling problem is equivalent to a contradirectional scattering problem in which the grating is excited from port 3 and the response monitored at port 4 (Figure 1). The main difference between the two cases is in the nature of the elements of the coupling matrix $M_C(\Delta,q)$, where the hyperbolic functions are now replaced by trigonometric functions. The coupling function q(z) can be calculated in a unique way if either the spectral response $H_{eq}(\beta)$ or, alternatively, the impulse response $h_{eq}(\tau)$, of this equivalent contradirectional problem are specified. As the spectral response $H_{eq}(\beta)$ is expressed in terms of the transfer functions $T_{SF}(\beta)$ and $T_{FF}(\beta)$:

$$H_{eq}(\beta) = \frac{T_{SF}(\beta)}{T_{FF}(\beta)} \ , \tag{11}$$

in order to determine the grating q(z) in a unique manner we must know both $T_{SF}(\beta)$ and $T_{FF}(\beta)$. Once a target spectral response $T_{SF}(\beta)$ has been specified, then the modulus $|T_{FF}(\beta)|$ can be calculated from the power conservation principle (7.3). However, there is certain freedom in the selection of its phase and, depending on this choice, several coupling functions q(z) that correspond to the same $T_{SF}(\beta)$ could be obtained. If we impose the additional constraint that the synthesised filter has to be undercoupled, then the phase of $T_{FF}(\beta)$ is uniquely determined by the minimum phase property of this function. This filter will be optimum in the sense that it gives the desired spectral response with a minimum value for $|q(z)|$. The calculation of the phase for $T_{FF}(\beta)$ from previous knowledge of its modulus and the assumption that it is a causal minimum-phase function is a well known mathematical problem, and its solution can easily be calculated to within an unimportant additive constant by means of the Hilbert transform [25,26].

3.2 The algorithm

We will present now a layer peeling algorithm that calculates the coupling function q(z) for an undercoupled GACC with an specified spectral response $T_{SF}(\beta)$. The first step will always be to obtain the modulus of the associated transfer function $T_{FF}(\beta)$ by means of the power conservation principle. Then, using the minimum phase property of $T_{FF}(\beta)$, we perform a Hilbert transform on $\log(|T_{FF}(\beta)|)$ to calculate its phase. Once we have both $T_{SF}(\beta)$ and $T_{FF}(\beta)$, we determine the spectral response of the equivalent contradirectional problem $H_{eq}(\beta)$ (11) and, subsequently, calculate the corresponding impulse time response $h_{eq}(\tau)$ by means of a Fourier transform.

The principle of the inverse scattering algorithm for the equivalent contradirectional problem relies on the synthesis of the impulse response $h_{eq}(\tau)$ in the time domain τ. In general, the impulse response $h_{eq}(\tau)$ can be calculated as a sum of the contributions of all the possible space-time (z,τ) propagation paths between the points (0,0) and $(0,\tau)$ (Figure 5). Notice that, for simplicity, we now measure distances (z) from the output port of the grating. Path #1 in this figure represents those paths with only one scattering event. Analogously, path #n represents those with 2n-1 scattering events. When the discretisation step Δ is very small $(\Delta \to 0)$. the impulse response at time τ can be written as:

$$h_{eq}(\tau) = -\frac{1}{2} q^{*}\left(\frac{\tau}{2}\right) + h_T(\tau) \qquad (12)$$

where $q(\tau/2)$ is the coupling function of the grating at $z=\tau/2$, and $h_T(\tau)$ is the impulse response at time τ for the same grating when is truncated at $z=(\tau/2)^{-}$. $h_T(\tau)$ accounts for light that has suffered multiple reflections within the grating, while $q^{*}(\tau/2)$ is the contribution of the direct propagation path #1. Equation (12) allows us to reconstruct the value of the coupling function $q(\bar{z})$ at each space point $\bar{z}$ from knowledge of both the impulse response $h_{eq}(\tau)$ at $\tau=2\bar{z}$ and the value of the coupling function $q(z)$ at previous $z<\bar{z}$ (i.e. $h_T(\tau)$). We have to stress that if the impulse response $h_T(\tau)$ of the truncated grating is calculated taking into account all the multiple reflections, then the reconstruction process is exact.

The grating coupling function $q(z)$ will be calculated following an analogous procedure to that developed in [21]. Let us assume that the first N layers of the grating $\{q(0),\ldots, q(N\Delta)\}$ have been obtained and, consequently, the accumulated transfer matrix $M_T^{-1}(N\Delta,\beta)$ is known (Figure 6). As the reconstruction process starts from the end of the grating, we will work with the inverse of the coupling, propagation and transfer matrices: $M_C^{-1}(\Delta, q(N\Delta))$, $M_P^{-1}(\Delta,\beta)$ and $M_T^{-1}(N\Delta,\beta)$ respectively. The impulse response $h_T(\tau)$ corresponding to $M_T^{-1}(N\Delta,\beta)$ will then match accurately the target impulse response $h_{eq}(\tau)$ for the time interval $[0, 2N\Delta]$. The steps to calculate the next coupling coefficient $q((N+1)\Delta)$ are as follows:

- From $M_T^{-1}(N\Delta,\beta)$ calculate the impulse response $h_T(\tau)$ of the truncated grating $[0, N\Delta]$ at $\tau = 2(N+1)\Delta$.
- Compute the difference $\Delta h(\tau)$ between the target impulse response $h_{eq}(\tau)$ and the truncated impulse response $h_T(\tau)$ at $\tau = 2(N+1)\Delta$.
- Calculate the adequate $q((N+1)\Delta)$ so as to match the impulse response $h_{eq}(\tau)$ at $\tau = 2(N+1)\Delta$ with the desired degree of accuracy. This involves solving the equation:

$$\Delta h(2(N+1)\Delta) = -\frac{q^*((N+1)\Delta)}{2}\frac{tg(|q((N+1)\Delta)|\cdot\Delta)}{|q((N+1)\Delta)|\cdot\Delta}\prod_{m=0}^{N}\left[\cos(|q(m\Delta)|\cdot\Delta)\right]^{-2}$$

(13)

which is the discrete counterpart of (12).

- Finally we should compute the new accumulated transfer function $M_T^{-1}((N+1)\Delta,\beta)$:

$$M_T^{-1}((N+1)\Delta,\beta) = M_C^{-1}(\Delta,q((N+1)\Delta))\cdot M_P^{-1}(\Delta,\beta)\cdot M_T^{-1}((N+1)\Delta,\beta) \quad (14)$$

and carry out the same sequence of steps to identify the next layer.

The complexity of the described algorithm scales as $O(N_{max}^2)$, where N_{max} is the maximum number of layers in the grating. The difference between the ideal target spectral response $T_{SF}(\beta)$ and that of the synthesised discrete grating is of the order $O(\Delta^2)$, where Δ is the step size of the discretisation grid. This error is negligible for small enough values of Δ.

From the discussion in Section 2.3 about the properties of the Z-transformed transfer function $T_{FF}(Z)$, we know that when the first of its zeros crosses the unit circle, the spectral response of the equivalent contradirectional problem $H_{eq}(\beta)$ (11) becomes infinite at the corresponding detuning β. The algorithm will not be able to converge in this limiting case. For this reason, the maximum coupled power between the two modes $|T_{SF}(\beta)|^2$ has to be kept below 1 in order to avoid convergence problems. The maximum permissible value for $|T_{SF}(\beta)|^2$ will depend on each case but, in general, can be very close to 1 (>0.95). If the spectral response of the filter is smooth enough, $|T_{SF}(\beta)|^2$ can be higher than 0.99.

4. Examples

We now illustrate the reconstruction and design of GACCs with several examples. Initially we will reconstruct a uniform grating from its analytical solution, proving the robustness of the method. Then we will design two filters with practical utility. Firstly, a band-pass filter with a top-flat transfer function; and secondly, a triangular filter for wavelength measurement of narrow-band optical signals.

4.1 Reconstruction of a uniform grating

In order to test the algorithm we will reconstruct the coupling function of a uniform grating from the analytical solution of its spectral response $T_{SF}(\beta)$ (8). Two different cases will be considered. First we will reconstruct an undercoupled uniform grating. As discussed in Section 3, our algorithm will be able to reconstruct accurately this undercoupled filter. Then, we will feed the inverse scattering algorithm with the spectral response $T_{SF}(\beta)$ of an overcoupled uniform grating. Now the algorithm will synthesise a grating with a nonuniform coupling function q(z) that corresponds to the same spectral response $T_{SF}(\beta)$, but yields an undercoupled realisation of the filter.

- **Undercoupled uniform GACC**

We will start by reconstructing an undercoupled uniform GACC from its analytical solution. The effective refractive index difference between the two interacting modes Δn_{eff} will be $3\cdot10^{-3}$ for all our examples. We consider a grating with a coupling constant q of 0.0283cm^{-1} and a length of 50cm. The transfer of power between the two modes at resonance $|T_{SF}(\beta)|^2$ is 0.975. Figure 7 shows the reconstructed coupling function, which matches very accurately that of the original uniform grating. Some Gibbs oscillations can be observed at the vicinity of the beginning and end of the grating.

- **Overcoupled uniform GACC and its undercoupled realisation**

Now we consider an overcoupled uniform grating with a coupling constant q of 0.0471cm^{-1} and a length of 50cm. The degree of overcoupling is 1, and its spectral response $T_{SF}(\beta)$ has a power coupling at resonance of 0.5 as can be observed in Figure 8a. Feeding this transfer function in our algorithm we find the coupling function q(z) of a nonuniform undercoupled GACC with identical response $T_{SF}(\beta)$ (Figure 8b). The original uniform overcoupled GACC also appears in Figure 8b for comparison purposes. The transfer functions of both gratings will only differ in the phase of $T_{FF}(\beta)$.

4.2 Design of a top-flat band-pass filter

To show the filter-design capability of the algorithm we will synthesise a grating with a top-flat spectral response, sharp band-edge transitions, and extremely low side lobes. The target filter has a flat band-pass of 1400GHz, with a raised-cosine shaped band edges that extended for 600GHz. These values are arbitrary, and the inverse scattering method could design sharper transitions at the expense of increasing the length of the grating. The power coupled between the two modes within the flat pass-band was 0.95, and the filter was designed to exhibit no dispersion within it.

The spectral response of the synthesised filter can be observed in Figure 9 together with the target spectral response. The side-lobes of the synthesised filter were below -80dB. The synthesised grating had a total length of 100cm and resembled very closely to a sinc function (Figure 10). In this figure we also observe that the coupling function is real and symmetric, in contrast to the corresponding case for contradirectional gratings, where the grating is asymmetric [21].

4.3 Design of a triangular filter

Finally, we will design a filter with a power-coupling spectral response that increases linearly with frequency. This filter could be useful to measure the wavelength of narrow band optical signals by monitoring the power distribution between the two output ports. The spectral band of the filter that exhibits linear dependence between frequency and coupling-ratio will extend for 2000GHz; and its high coupling efficiency edge was smoothed by a raised cosine function that extended for 300GHz (Figure 11). The maximum power coupling efficiency for the filter will be 0.95, and it was designed again to have no dispersion along the whole spectral band.

Figure 11 shows the spectral response of the synthesised filter and compares it with the ideal target. We observe again very low side-lobes (<-80dB) and good agreement between both sets of curves. The coupling function of the designed grating q(z) can be observed in Figure 12. Due to the asymmetric spectral response of the filter, q(z) is a complex function, with its real part being symmetric, and its imaginary part antisymmetric. In order to fabricate this GACC, an accurate control of both the modulus and phase of the coupling coefficient q(z) will be necessary.

5. Conclusions

This paper has presented an efficient inverse scattering algorithm for the design of grating assisted codirectional couplers with a specified spectral response $T_{SF}(\beta)$ for the coupling between the two interacting modes. We have shown that the transfer function $T_{FF}(\beta)$ for the uncoupled light does not satisfy in general the minimum-phase property and, in consequence, the inverse scattering solution can be non-unique. The different solutions will differ on the phase of the $T_{FF}(\beta)$ transfer function. The solution of the inverse scattering problem can be uniquely determined if we add the requirement of minimum-phase for the transfer function $T_{FF}(\beta)$. The gratings designed with this constraint will be optimum in the sense that they are undercoupled realisations of the target filter, yielding minimum values for the coupling function q(z). Once both $T_{SF}(\beta)$ and $T_{FF}(\beta)$ are known, the calculation of q(z) can be carried out in an analogous way as in the case of contradirectional inverse scattering. We have defined an equivalent contradirectional problem and applied a fast layer peeling method for its solution. The method has been illustrated by reconstructing uniform gratings, and by designing top-flat filters and filters with linear frequency dependence. For all the cases, the agreement between the target and synthesised spectral responses was very satisfactory.

References

[1] A. Yariv. "Coupled-mode theory for guided-wave optics". IEEE Journal of Quantum Electronics, Vol. 9, No.9, pp. 919-933. September, 1973.

[2] D. Marcuse. "Directional couplers made of nonidentical asymmetric slabs. Part II: grating assisted couplers". Journal of Lightwave Technology, Vol. 5, No. 2, pp. 268-273. February, 1987.

[3] W.P. Huang. "Coupled-mode theory for optical waveguides: an overview". Journal Optical Society of America A, Vol. 11, No. 3, pp. 963-983. March, 1994.

[4] G. Meltz, W.W. Morey, W.H. Glen. "Formation of Bragg gratings in optical fibres by a transverse holographic method". Optics Letters, Vol. 14, No.15, pp. 823-825. August, 1989.

[5] A.M. Vengsarkar, J.R. Pedrazzani, J.B. Judkins, P.J. Lemaire, N.S. Bergano, C.R. Davidson. "Long-period fiber-grating-based gain equalisers". Optics Letters, Vol. 21, No. 5, pp. 336-338. March 1996.

[6] P.St.J. Russell, D. P. Hand. "Rocking filter formation in photosensitive high birefringence optical fibres". Electronics Letters Vol. 26, No. 22, pp. 1846-1848, October 1990.

[7] J.N. Blake, B.Y. Kim. H.E. Engan, H.J. Shaw. "Analysis of intermodal coupling in a two-mode fiber with periodic microbends". Optics Letters, Vol. 12, No. 4, pp. 281-283. April 1987.

[8] K.I. Hopcraft, P.R. Smith. "An introduction to electromagnetic inverse scattering". Kluwer Academic Publishers. Netherlands, 1992.

[9] J.A. Dobrowolski, D. Lowe "Optical thin film synthesis program based on the use of Fourier transforms". Applied Optics, Vol. 17, No. 19, pp. 3039-3050. October, 1978.

[10] B.G. Bovard. "Fourier transform technique applied to quarterwave optical coatings". Applied Optics, Vol. 27, No. 15, pp. 3062-3063. August, 1988.

[11] K.A. Winick, J.E. Roman. "Design of corrugated waveguide filters by Fourier-transform techniques". IEEE Journal of Quantum Electronics, Vol. 26, No.11, pp. 1918-1929. November, 1990.

[12] I.M. Gel'fand, B.M. Levitan. "On a determination of a differential equation from its spectral function". Amer. Math. Soc. Trasl., Ser. 2, Vol. 1, pp. 253-304. (1955)

[13] I. Kay. "The inverse scattering problem when the reflection coefficient is a rational function". Communications in Pure and Applied Mathematics, Vol. 13, pp. 371-393. (1960)

[14] G.H. Song, S.Y. Shin. "Design of corrugated waveguide filters by the Gel'fan-Levitan-Marchenko inverse-scattering method". Journal of the Optical Society of America A, Vol. 2, No.11, pp. 1905-1915. November, 1985.

[15] J.E. Roman, K.A. Winick. "Waveguide grating filters for dispersion compensation and pulse compression". IEEE Journal of Quantum Electronics, Vol. 29, No.3, pp. 975-982. March, 1993.

[16] E. Peral, J. Capmany, J. Marti. "Iterative solution to the Gel'fan-Levitan-Marchenko coupled equations and application to synthesis of fiber gratings". IEEE Journal of Quantum Electronics, Vol. 32, No.12, pp. 2078-2084. December, 1996.

[17] B.E. Little, C. Wu, W.P. Huang. "Synthesis of codirectional couplers with ultralow sidelobes and minimum bandwidth". Optics Letters, Vol. 20, No. 11, pp. 1259-1261. June, 1995.

[18] J. Skaar, K.M. Risvik. "A genetic algorithm for the inverse problem in synthesis of fiber gratings". Journal of Lightwave Technology, Vol. 16, No. 10, pp. 1928-1932. October, 1998.

[19] A.M. Bruckstein, B.C. Levy, T. Kailath. "Differential methods in inverse scattering". SIAM J. Appl. Math. , Vol. 45, No. 2, pp. 312-335. April, 1995.

[20] A.M. Bruckstein, T. Kailath. "Inverse scattering for discrete transmission-line models". SIAM Review, Vol. 29, No. 3, pp. 359-389. September, 1987.

[21] R. Feced, M.N. Zervas, M.A. Muriel. "An efficient inverse scattering algorithm for the design of nonuniform fibre Bragg gratings". To be published IEEE Journal of Quantum Electronics. August, 1999.

[22] H. Kogelnik, C.V. Shank. "Coupled-wave theory of distributed feedback lasers". Journal of Applied Physics, Vol. 43, No. 5, pp. 2327-2335. May, 1972.

[23] J.G. Proakis, D.G. Manolakis. "Introduction to digital signal processing". McMillan Publishing Company. New York, 1988.

[24] E.M. Dowling, D.L. MacFarlane. "Lightwave lattice filters for optically multiplexed communication systems". Journal of Lightwave Technology, Vol. 12, No. 3, pp. 471-486. March, 1994.

[25] A.B. Carlson. "Communication systems", pp. 103-105. McGraw-Hill International Edition. Singapore, 1986.

[26] L. Mandel, E. Wolf. "Optical coherence and quantum optics", pp. 92-108, 384-388. Cambridge University Press, 1995.

Figure Captions

Figure 1. Grating-Assisted Codirectional Coupler. F: Fast mode, S: Slow Mode.

Figure 2. Space-time paths corresponding to the propagation of two coupled modes through a grating as described by equation (4) and lattice digital-filter model for the discrete GACC.

Figure 3. Space-time paths corresponding to the propagation through the grating of two coupled modes when time-delays are measured with respect to the fast mode and the corresponding lattice digital-filter model for the discrete GACC.

Figure 4. Zero-diagram in the complex plane for the $T_{FF}(Z)$ transfer function of a uniform GACC for the following values of the product qL: $10^{-150} \cdot (\pi/2)$, $0.5\cdot(\pi/2)$, $1\cdot(\pi/2)$, $2\cdot(\pi/2)$, $3\cdot(\pi/2)$, and $8\cdot(\pi/2)$.

Figure 5. Space-time diagram for the equivalent contradirectional problem. #n represents those paths with 2n-1 scattering events.

Figure 6. Space-time diagram that illustrates the reconstruction process of the equivalent contradirectional problem for the discretised GACC.

Figure 7. Reconstruction of a uniform grating with a q of $0.0283 cm^{-1}$ and a length of 50cm: —, reconstructed grating; ····, original grating.

Figure 8. Undercoupled realisation of a uniform overcoupled grating with a q of $0.0471 cm^{-1}$ and a length of 50cm. **(a)** Spectral response $|T_{SF}(\beta)|^2$. **(b)** Coupling function q(z): —, undercoupled grating; ····, overcoupled grating.

Figure 9. Spectral response $|T_{SF}(\beta)|^2$ of the synthesised top-flat filter in linear and logarithmic scales.

Figure 10. Coupling function q(z) of the synthesised top-flat filter.

Figure 9. Spectral response $|T_{SF}(\beta)|^2$ of the synthesised triangular filter in linear and logarithmic scales.

Figure 10. Real and imaginary part of the coupling function q(z) that corresponds to the synthesised triangular filter.

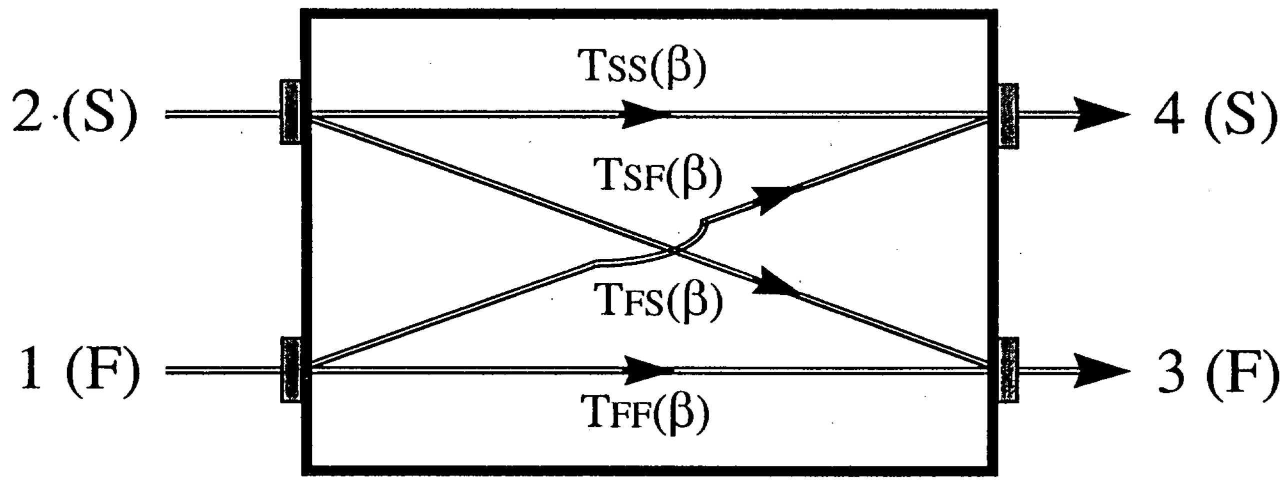
2 (S)
1 (F)
TSS(β)
TSF(β)
TFS(β)
TFF(β)
4 (S)
3 (F)

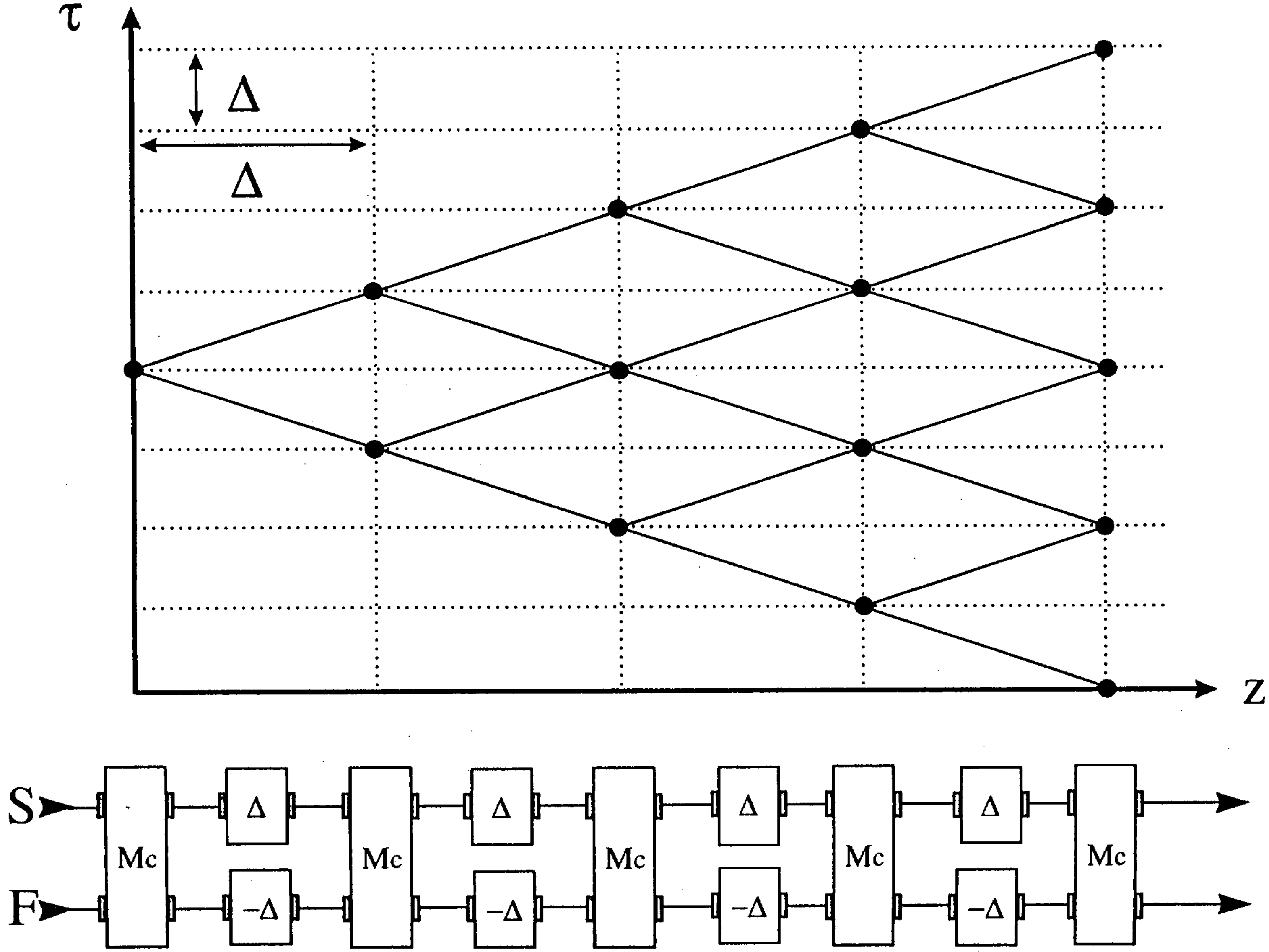
τ
Δ
Δ
z
S
F
Mc
Δ
−Δ

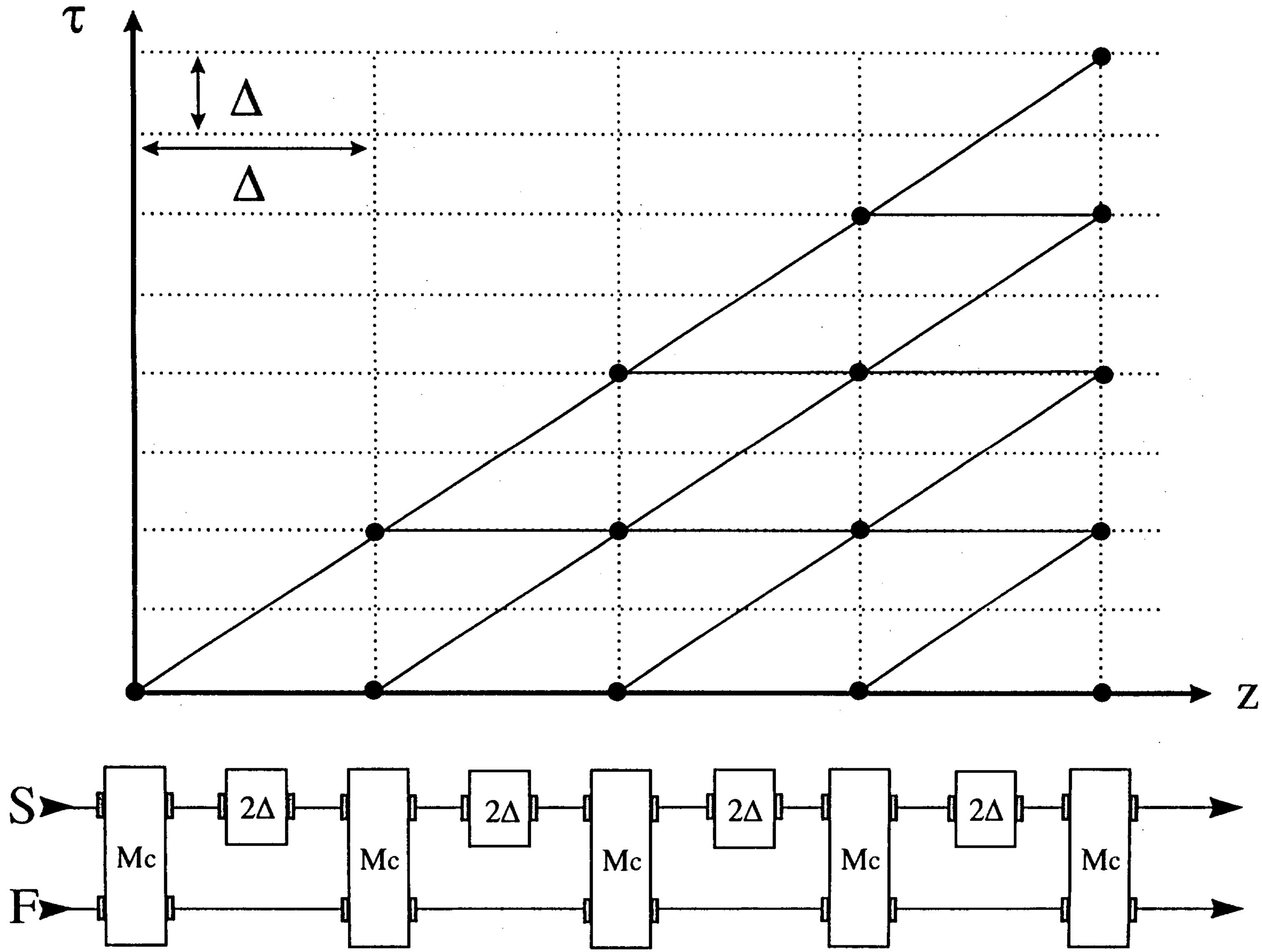
τ
Δ
Δ
z
S
F
Mc
2Δ
Mc
2Δ
Mc
2Δ
Mc
2Δ
Mc

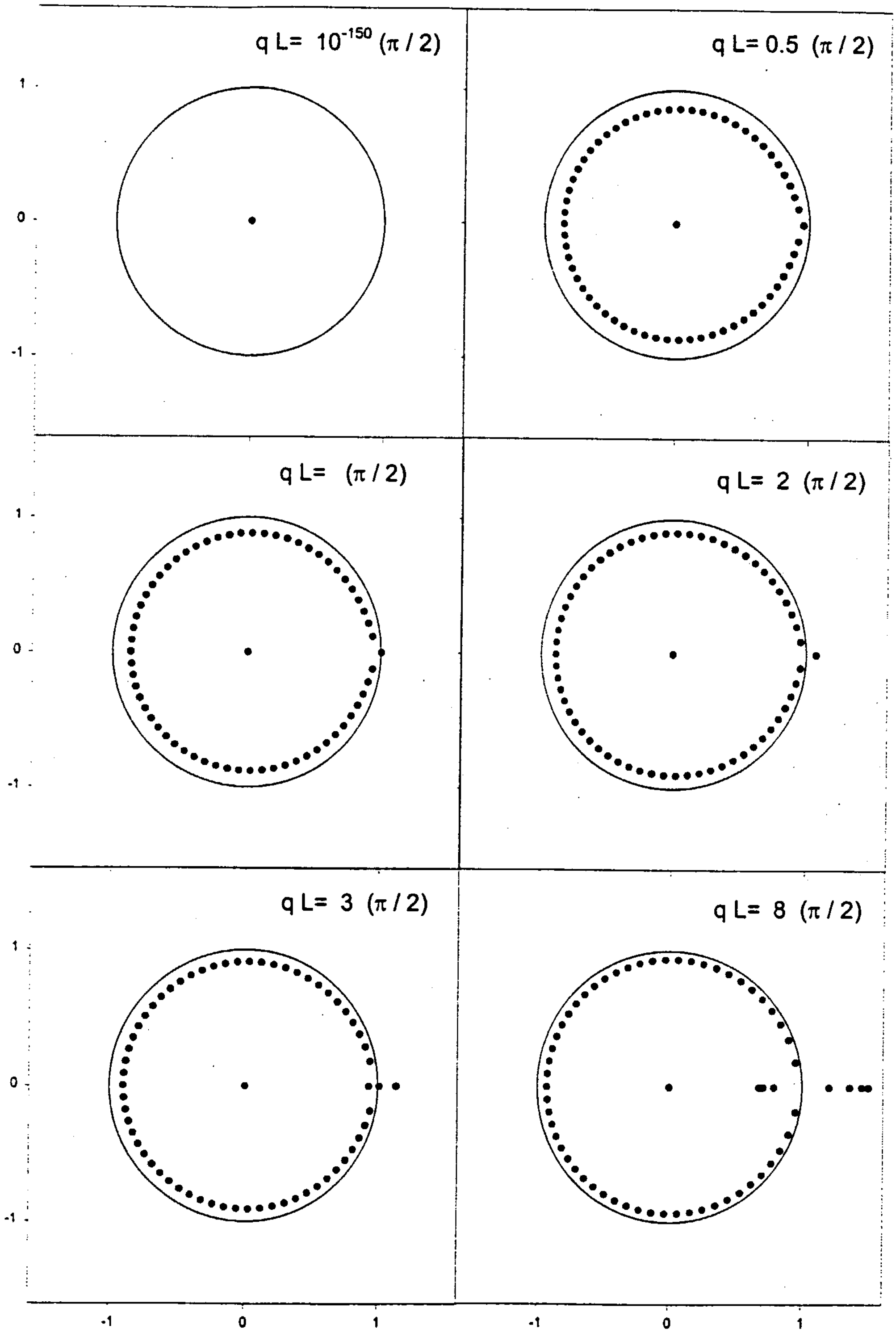
q L= 10^{-150} (π / 2)
q L= 0.5 (π / 2)
q L= (π / 2)
q L= 2 (π / 2)
q L= 3 (π / 2)
q L= 8 (π / 2)
1
0
-1
-1
0
1

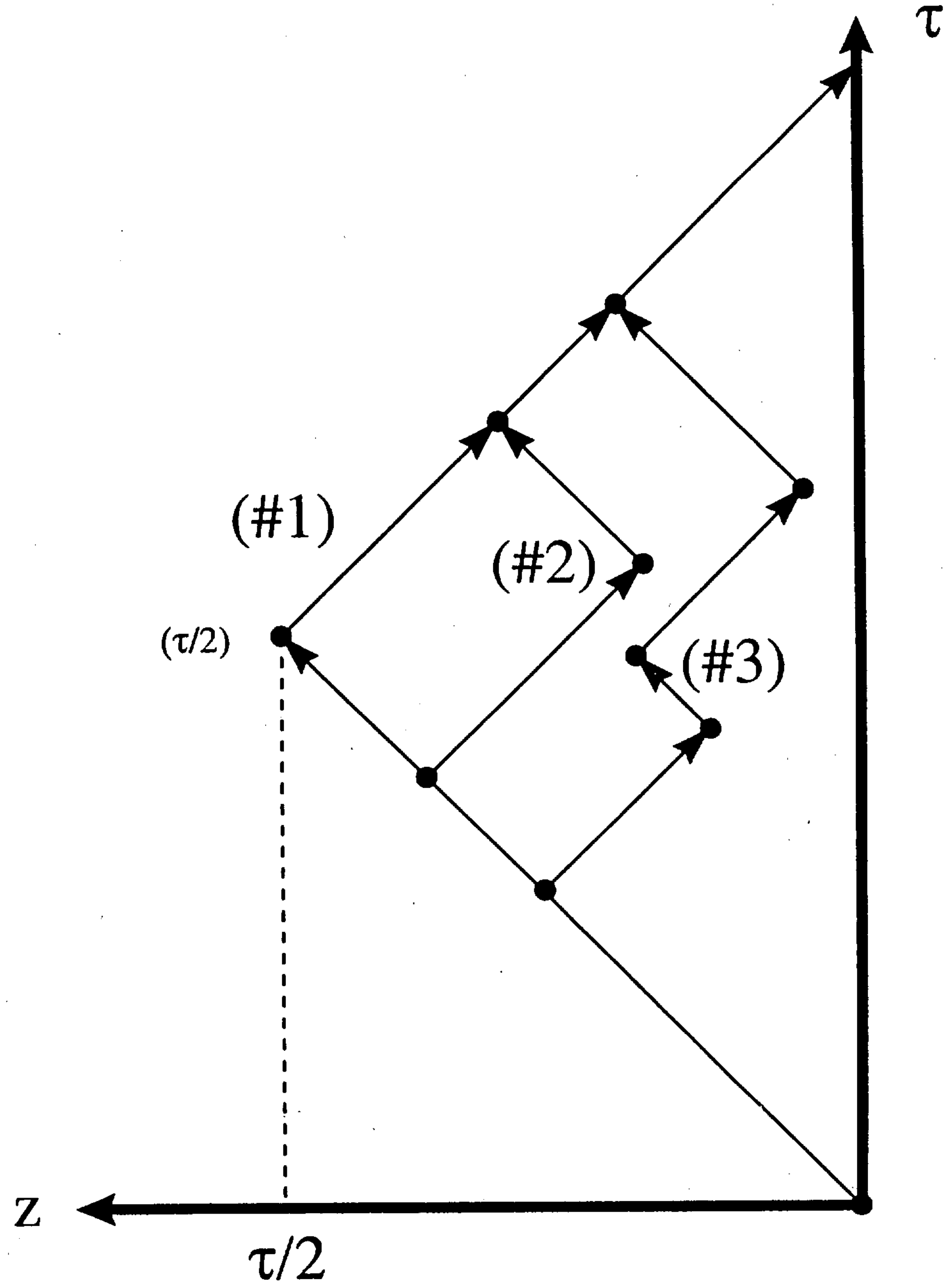
τ
(#1)
(#2)
(#3)
(τ/2)
z
τ/2

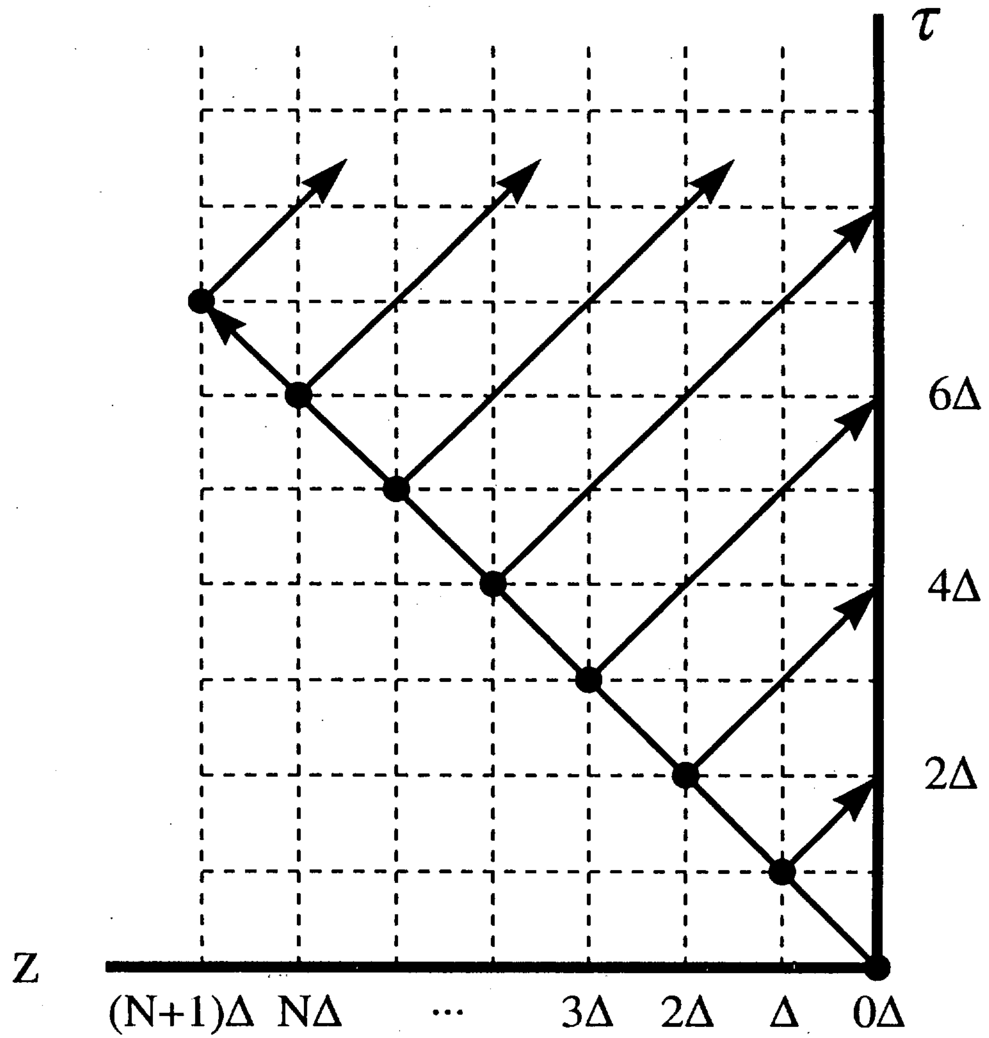
τ
6Δ
4Δ
2Δ
Z
(N+1)Δ NΔ
...
3Δ
2Δ
Δ
0Δ

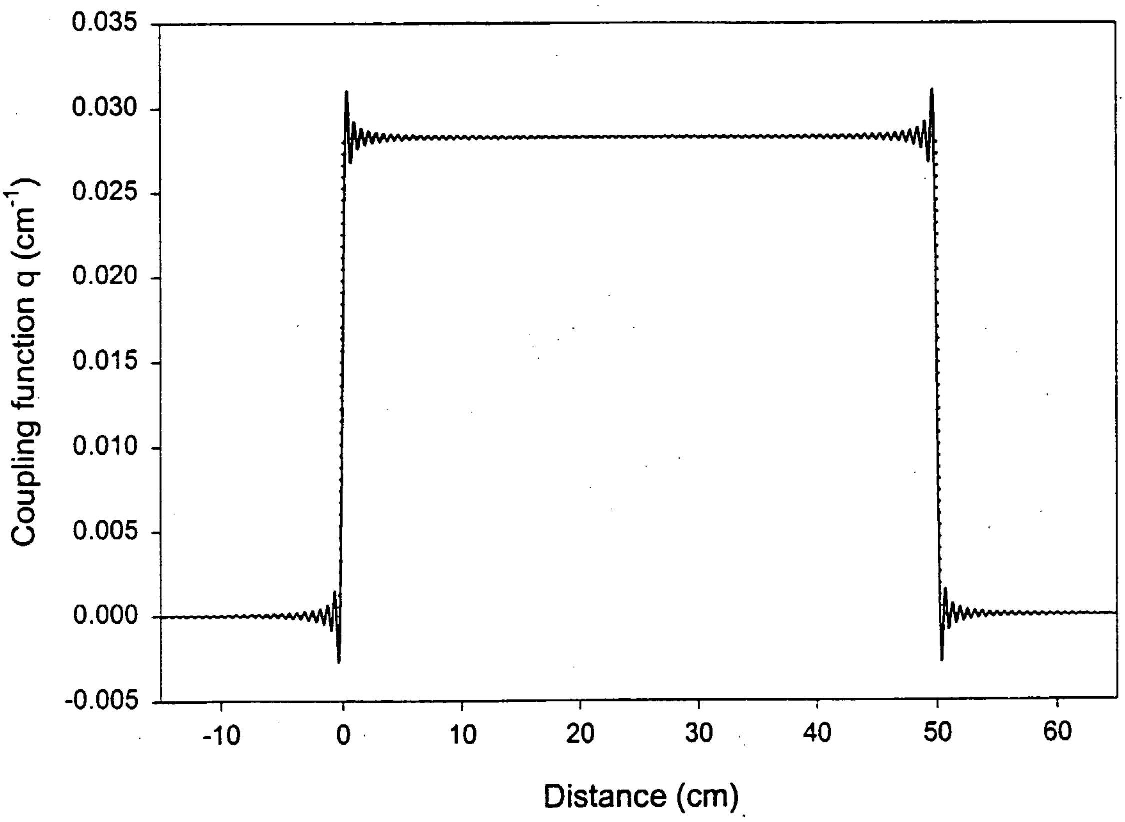

0.035
0.030
0.025
0.020
0.015
0.010
0.005
0.000
-0.005
Coupling function q (cm-1)
-10
0
10
20
30
40
50
60
Distance (cm)

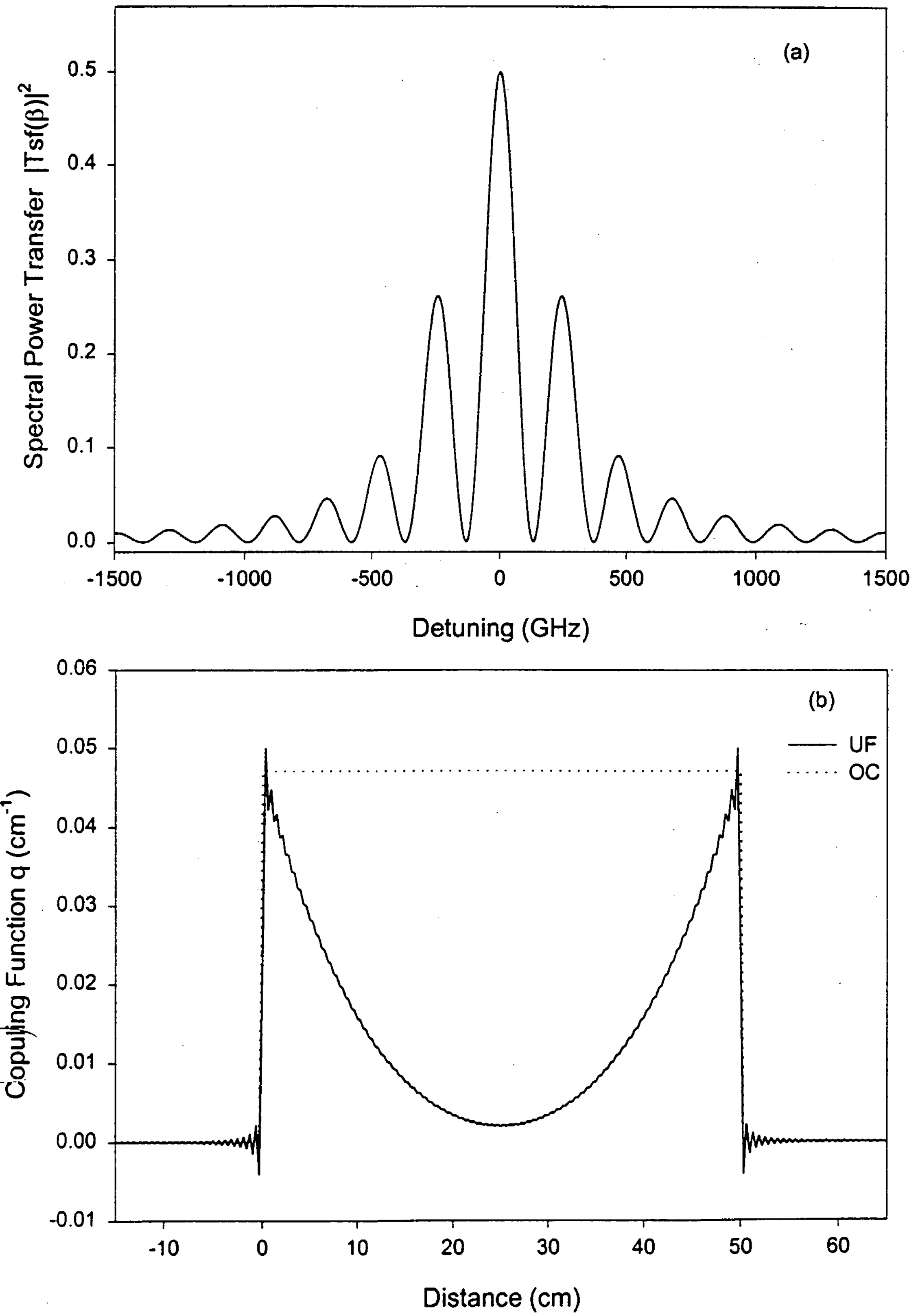
(a)
Spectral Power Transfer |Tsf(β)|²
0.0
0.1
0.2
0.3
0.4
0.5
-1500
-1000
-500
0
500
1000
1500
Detuning (GHz)
(b)
UF
OC
Copuling Function q (cm⁻¹)
-0.01
0.00
0.01
0.02
0.03
0.04
0.05
0.06
-10
0
10
20
30
40
50
60
Distance (cm)

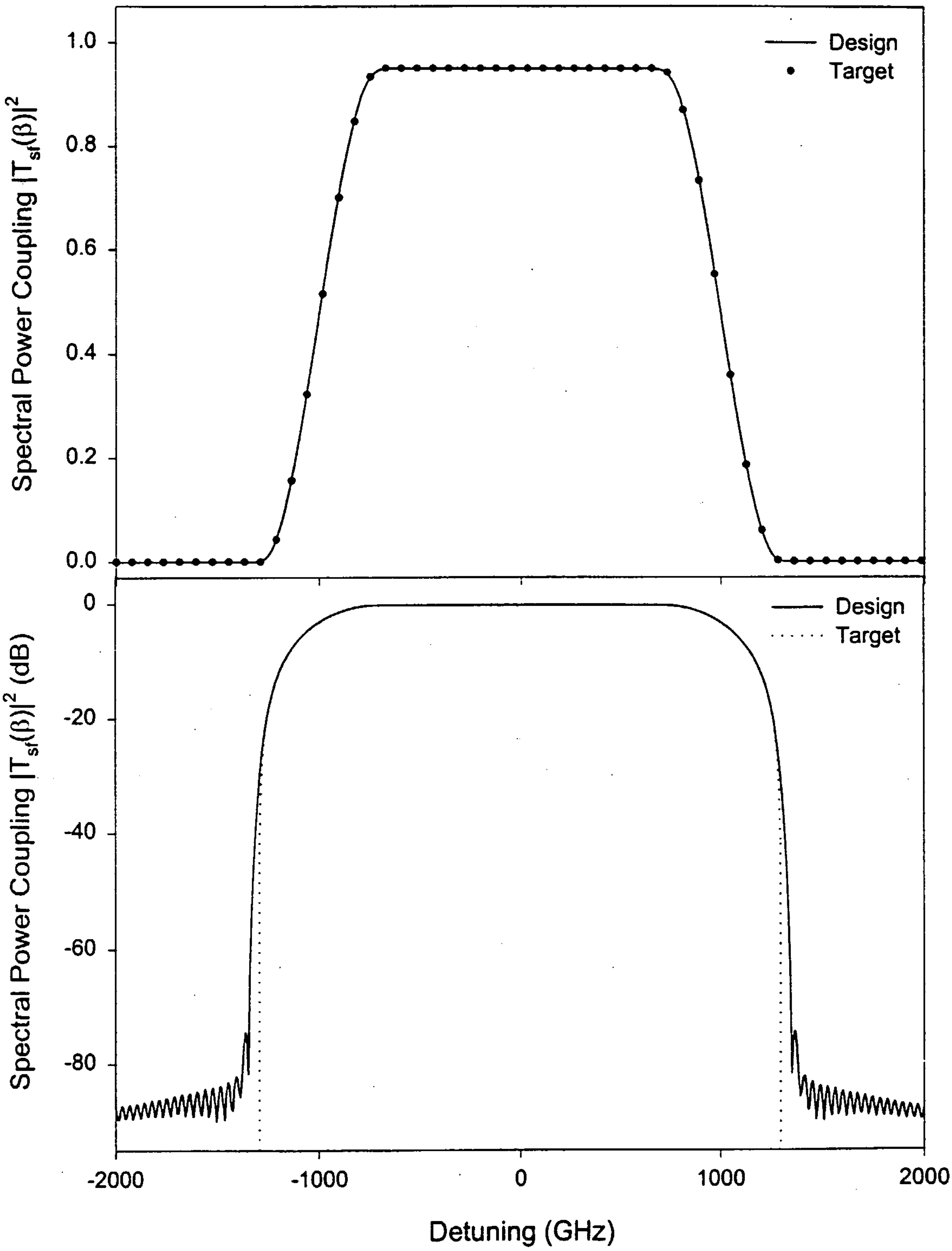
Design
Target
Spectral Power Coupling $|T_{sf}(\beta)|^2$
1.0
0.8
0.6
0.4
0.2
0.0
Design
Target
Spectral Power Coupling $|T_{sf}(\beta)|^2$ (dB)
0
-20
-40
-60
-80
-2000
-1000
0
1000
2000
Detuning (GHz)

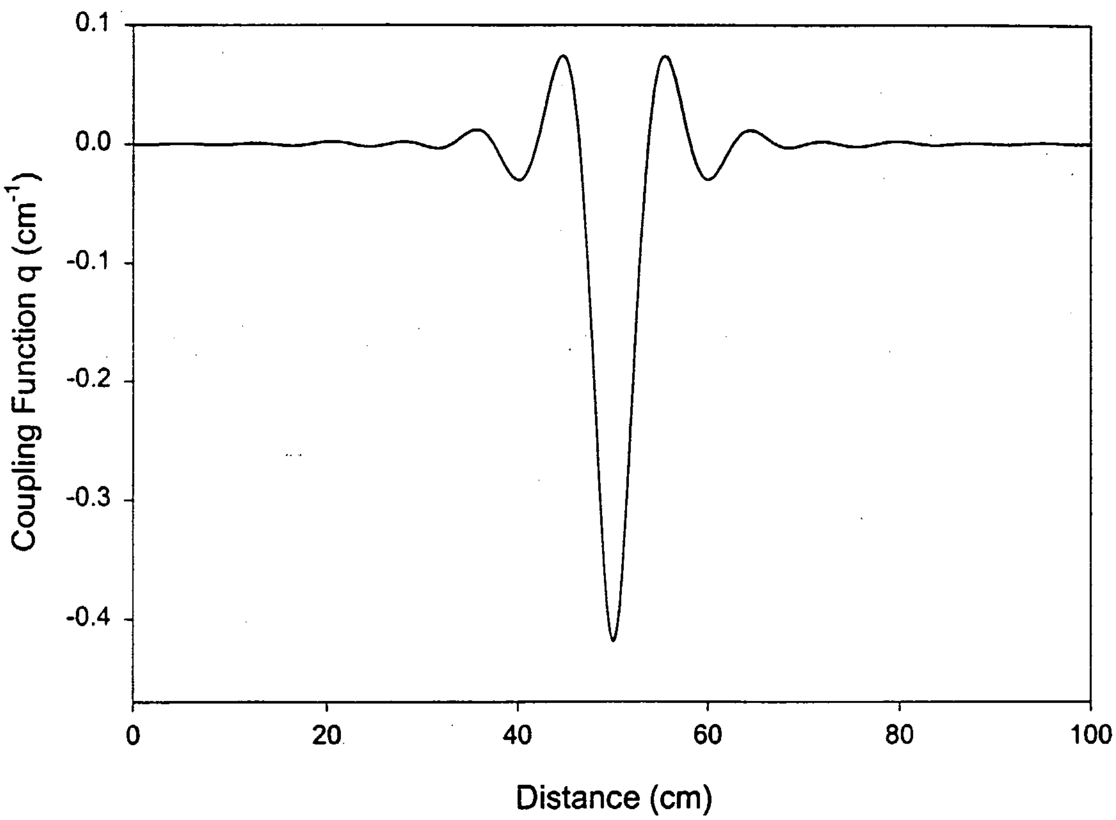

0.1
0.0
-0.1
-0.2
-0.3
-0.4
Coupling Function q (cm^{-1})
0
20
40
60
80
100
Distance (cm)

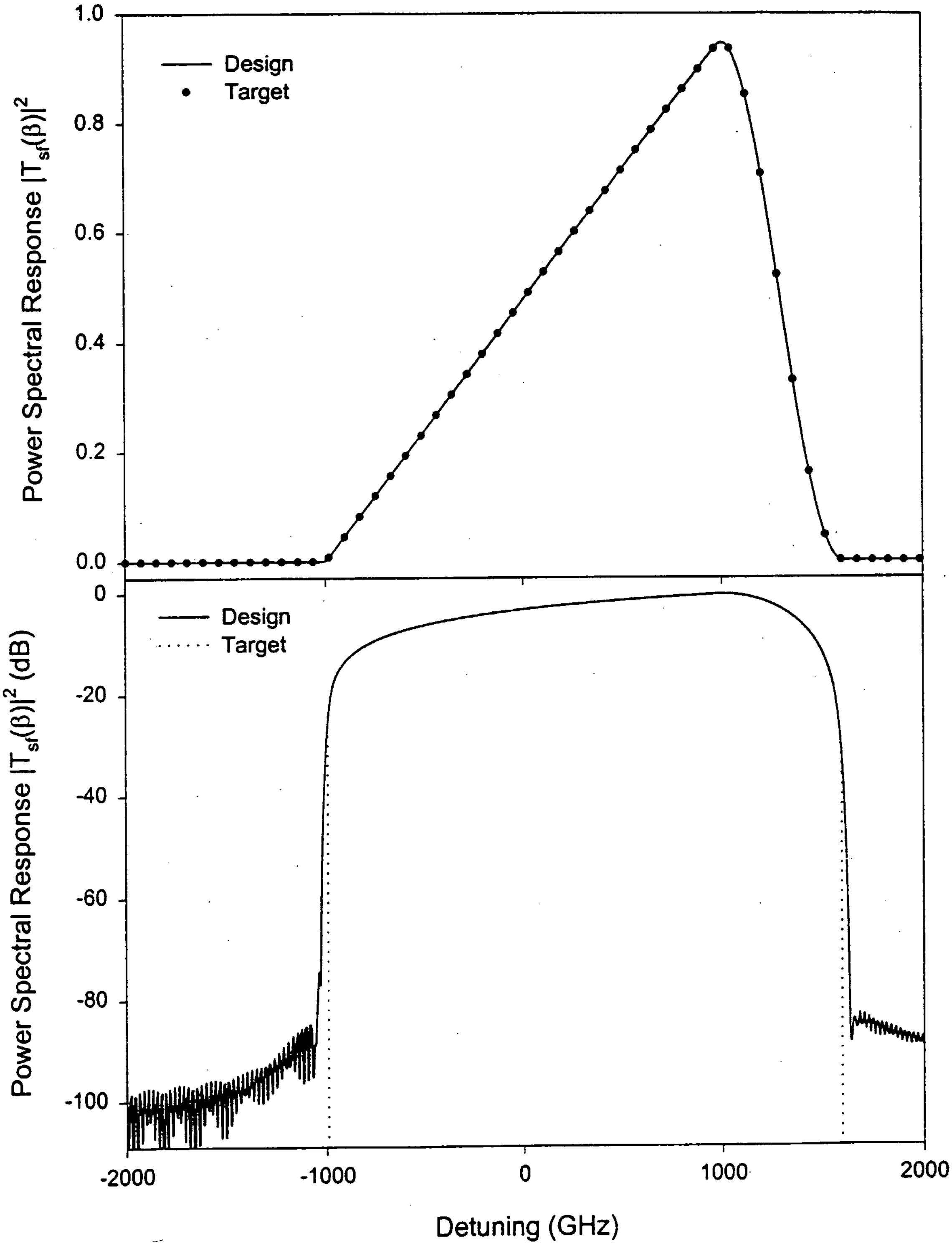
Design
Target
Power Spectral Response $|T_{sf}(\beta)|^2$
1.0
0.8
0.6
0.4
0.2
0.0
Design
Target
Power Spectral Response $|T_{sf}(\beta)|^2$ (dB)
0
-20
-40
-60
-80
-100
-2000
-1000
0
1000
2000
Detuning (GHz)

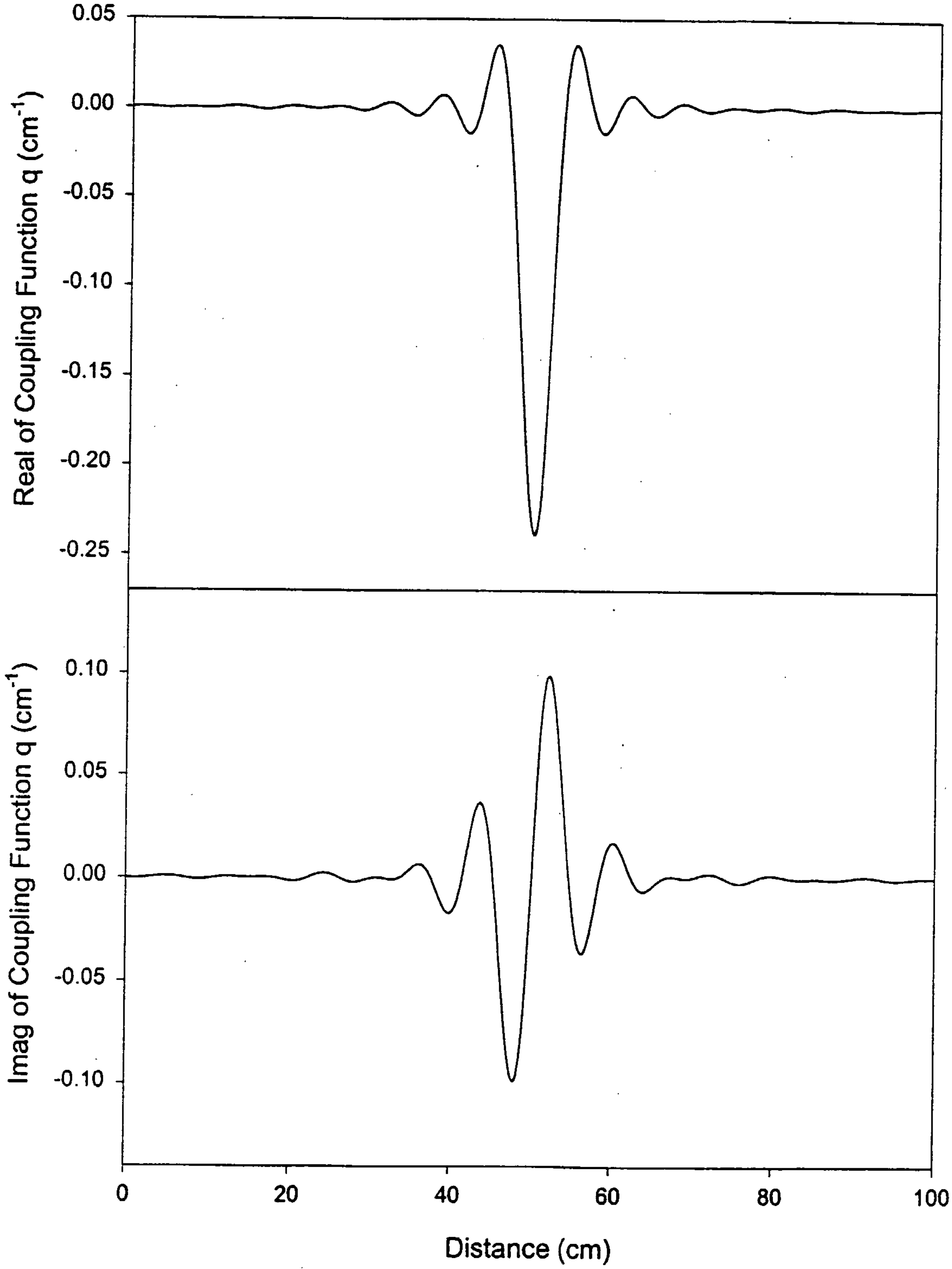

Real of Coupling Function q (cm^{-1})
0.05
0.00
-0.05
-0.10
-0.15
-0.20
-0.25
Imag of Coupling Function q (cm^{-1})
0.10
0.05
0.00
-0.05
-0.10
0
20
40
60
80
100
Distance (cm)